Physiological Measurement

IPEM
Institute of Physics and Engineering in Medicine

NOTE • OPEN ACCESS

The hemodynamic cardiac profiler volume-time curves and related parameters: an MRI validation study

To cite this article: Maurits K Konings *et al* 2024 *Physiol. Meas.* **45** 01NT01

IOP Publishing Physiol. Meas. 45 (2024) 01NT01 https://doi.org/10.1088/1361-6579/ad13af

Physiological Measurement

IPEM Institute of Physics and Engineering in Medicine

NOTE

The hemodynamic cardiac profiler volume-time curves and related parameters: an MRI validation study

Maurits K Konings[1,*], **Manuella Al Sharkawy**[4], **Sjoerd M Verwijs**[2], **Adrianus J Bakermans**[3], **Martijn Visscher**[4], **Charles L Hollenkamp**[4], **Denise P Veelo**[2] and **Harald T Jørstad**[2]

[1] Department of Medical Technology, University Medical Center Utrecht (UMCU), The Netherlands
[2] Department of Cardiology, Amsterdam University Medical Centers, location AMC, Amsterdam, The Netherlands
[3] Department of Radiology and Nuclear Medicine, Amsterdam University Medical Centers, University of Amsterdam, Amsterdam, The Netherlands
[4] The Surgical Company, Hemologic B.V., Amersfoort, The Netherlands
[*] Author to whom any correspondence should be addressed.

E-mail: m.konings@umcutrecht.nl

Keywords: hemodynamic cardiac profiler, cardiac magnetic resonance, volume time curve, systolic time, diastolic function, cardiac performance, heart monitoring

OPEN ACCESS

RECEIVED
29 May 2023

REVISED
14 November 2023

ACCEPTED FOR PUBLICATION
8 December 2023

PUBLISHED
10 January 2024

Abstract

Background. The hemodynamic cardiac profiler (HCP) is a new, non-invasive, operator-independent screening tool that uses six independent electrode pairs on the frontal thoracic skin, and a low-intensity, patient-safe, high-frequency applied alternating current to measure ventricular volume dynamics during the cardiac cycle for producing ventricular volume-time curves (VTCs). *Objective.* To validate VTCs from HCP against VTCs from MRI in healthy volunteers. *Approach.* Left- and right-ventricular VTCs were obtained by HCP and MRI in six healthy participants in supine position. Since HCP is not compatible with MRI, HCP measurements were performed within 20 min before and immediately after MRI, without intermittent fluid intake or release by participants. Intraclass correlation coefficients (ICCs) were calculated to validate HCP-VTC against MRI-VTC and to assess repeatability of HCP measurements before and after MRI. Bland–Altman plots were used to assess agreement between relevant HCP- and MRI-VTC-derived parameters. Precision of HCP's measurement of VTC-derived parameters was determined for each study participant by calculating the coefficients of variation and repeatability coefficients. *Main results.* Left- and right-ventricular VTC ICCs between HCP and MRI were >0.8 for all study participants, indicating excellent agreement between HCP-VTCs and MRI-VTCs. Mean (range) ICC of HCP right-ventricular VTC versus MRI right-ventricular VTC was 0.94 (0.88–0.99) and seemed to be slightly higher than the mean ICC of HCP left-ventricular VTC versus MRI-VTC (0.91 (0.80–0.96)). The repeatability coefficient for HCP's measurement of systolic time (tSys) was 45.0 ms at a mean value of 282.9 $\pm$ 26.3 ms. Repeatability of biventricular HCP-VTCs was excellent (ICC 0.96 (0.907–0.995)). *Significance.* Ventricular volume dynamics measured by HCP-VTCs show excellent agreement with VTCs measured by MRI. Since abnormal tSys is a sign of numerous cardiac diseases, the HCP may potentially be used as a diagnostic screening tool.

1. Introduction

Left- (LV) and right-ventricular (RV) systolic and diastolic volume dynamics constitute some of the most important parameters in cardiology (Göransson *et al* 2018). Over the past decades, cardiac magnetic resonance imaging (MRI) has developed into a powerful tool for quantification of heart chamber volume dynamics, surpassing echocardiography in accuracy and precision in a number of fields (Lima and Desai 2004). However, both echocardiography and MRI have inherent drawbacks. Costs, safety, complexity and measurement or processing time constitute important limitations of MRI (Mendoza *et al* 2010, Barison *et al* 2022).

Echocardiography, on the other hand, is implemented in most routine cardiological care, but is highly operator dependent and patient dependent (e.g. presence of adequate echocardiography windows) (Reant *et al* 2010). Hence, neither modality is suited for large-scale screenings comparable with electrocardiograms (ECG) or stethoscope auscultation. Therefore, there is an unmet need for easy-to-use screening devices that reliably quantify cardiac ventricular volume dynamics.

As previously demonstrated, the 'Hemodynamic Cardiac Profiler' (HCP) is able to measure volume-time curves (VTCs) of the ventricles (i.e. the volume of the blood inside the ventricles *as function of time* during a *single* cardiac cycle) in a wide range of settings (Konings *et al* 2012, Konings *et al* 2017). The HCP is a low-cost, non-invasive system, specifically designed to be easy to use, and requires no trained operator for its operation, i.e. the only training needed being following instructions for the application of a patch of skin electrodes. Hence, the HCP could potentially serve as an easy-to-use screening device.

In short, the principle of operation of the HCP is based on specific 2D-spatial voltage patterns on the thoracic skin related to either atrial or small ventricular volume changes, in combination with measured changes in a weak, patient-safe, applied alternating current field during the cardiac cycle (see Konings *et al* (2012) for details). Up to now, the HCP has not been validated against MRI, i.e. the current non-invasive gold standard to assess ventricular VTCs. We have previously demonstrated that an older HCP prototype (HCP prototype1, in use 2009–2017) was able to produce values for e.g. ratios of the volumes of early (*E*) and late (*A*) diastolic filling (*E*/*A* ratio), and that these values showed strong correlations with 2D transthoracic echocardiography (2D TTE) measurements at rest (Konings *et al* 2017). Nevertheless, echocardiography has significant limitations as a reference technique, and, most notably, is not suited for the validation of the VTCs themselves because the generation of VTCs using echocardiography is prone to significant inter-operator variability.

Here, we present a pilot validation and repeatability (i.e. accuracy and precision) study, aiming at a first validation of the VTCs measured by the current and improved HCP prototype2 (in use from 2017), against MRI-VTCs from left and right ventricles. Previously, the HCP system was not designed to distinguish between left-ventricular VTC (LV-VTC) and right-ventricular VTC (RV-VTC), and each VTC was simply considered to be the average of the LV-VTC and RV-VTC i.e. a biventricular VTC. The HCP prototype2 described in this paper is capable of extracting both LV-VTC and RV-VTC (from the biventricular VTC data) in healthy participants.

Furthermore, clinically relevant parameters such as systolic time (tSys), one-third filling fraction (1/3FF), and *E*/*A* ratio were derived from the VTCs produced by HCP and compared with their MRI-VTC counterparts.

2. Materials and methods

In this pilot validation and repeatability study, left-ventricular (LV) and right-ventricular (RV) VTCs were measured by both HCP and MRI in 6 healthy volunteers free from cardiovascular disease. The study protocol was approved by the Medical Ethics Committee of Amsterdam University Medical Centers (NL60812.018.17) and conducted according to the principles outlined in the Declaration of Helsinki (2013). Written informed consent was obtained from all study participants.

2.1. Study outcomes

Our primary outcome for HCP measurement *accuracy* was (a) agreement between HCP- and MRI-VTCs (one VTC per technique) per participant, as measured with intraclass correlation coefficients (ICCs), as well as (b) agreement assessed with Bland–Altman analyses between three VTC-derived parameters (tSys, 1/3FF, and *E*/*A* ratio) produced by HCP and by MRI. Furthermore, our primary HCP outcome for HCP measurement *precision* was (a) agreement (of the morphology) of three pairs of individual biventricular VTCs of HCP1 (pre-MRI) and HCP2 (post-MRI) measurements, assessed using ICCs, and (b) agreement between values (mean $\pm$ SD) for tSys and 1/3FF (and heart rate) of measurement HCP1 and HCP2.

2.2. HCP measurements

The current HCP system (prototype2) consists of two separate parts: the portable patient unit and the healthcare professional console. The patient carries the small, light-weight portable patient unit (dimensions: 20 cm $\times$ 15 cm $\times$ 5 cm) that is attached to a belt around the hips of the patient (figure 1(a)). The patient unit processes voltage signals from six independent electrode pairs from a disposable electrode patch on the skin of the patient (figure 1(b)). The healthcare professional console consists of a computer and a screen where the HCP measurements are displayed (figure 1(c)). The console computer is connected to the portable patient unit via a continuous Bluetooth connection. In comparison to the previously described system (prototype1) (Konings *et al* 2017), the current HCP protoype2 includes miniaturized electronics producing output that is less prone to electric disturbances. Furthermore, in contrast to prototype1, the wearable nature of prototype2 enlarges its

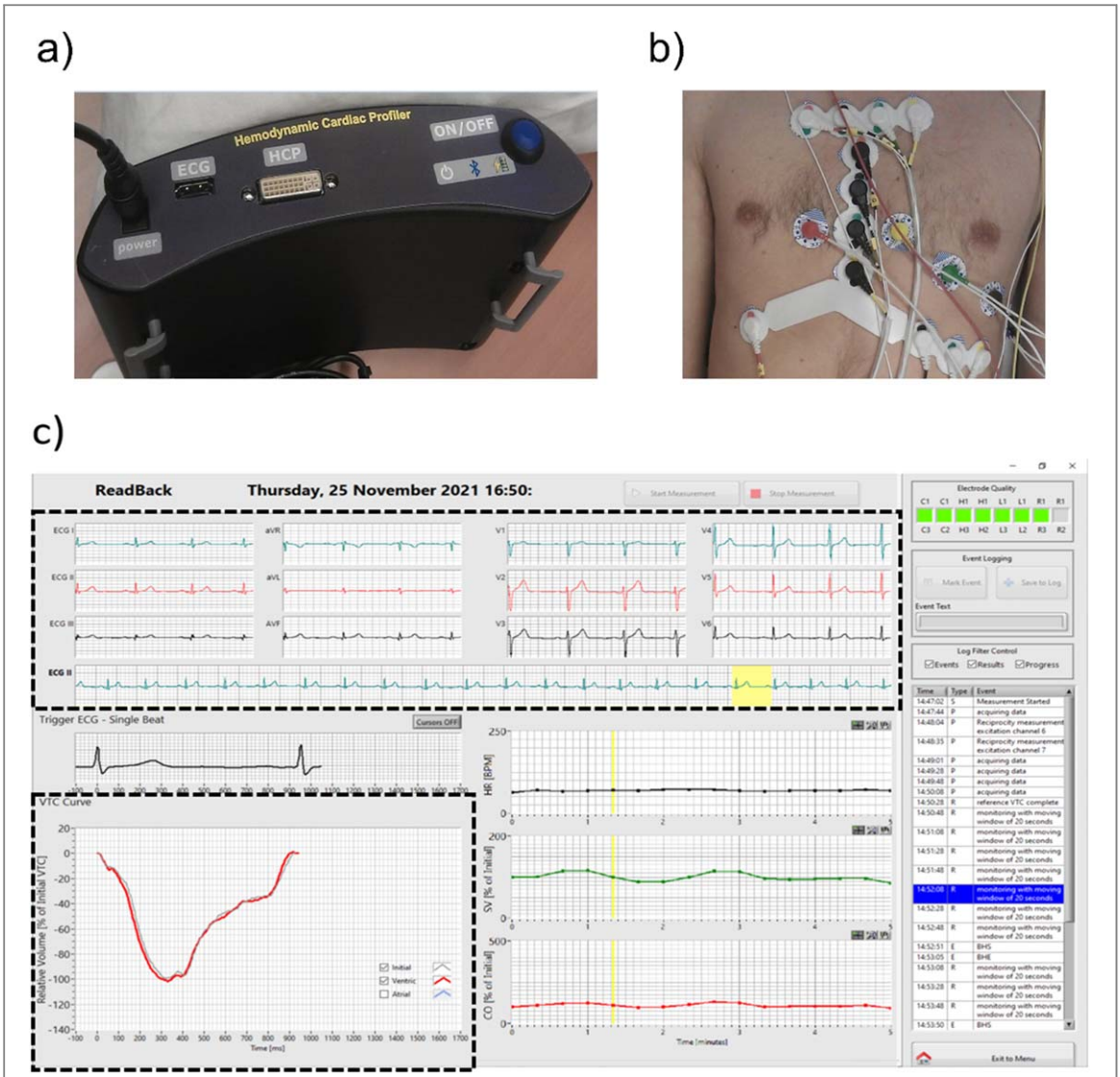

Figure 1. (a) Portable Hemodynamic Cardiac Profiler (HCP) patient unit (dimensions: 20 cm × 15 cm × 5 cm) that can be carried with a belt wrapped around the hips. (b) Disposable electrode patch (white), together with separate ECG electrodes (coloured) at standard 12-lead ECG positions. The HCP patient unit processes the signals from the electrode patch, and sends the data, via a continuous Bluetooth connection, to a separate console for the healthcare professional. This console consists of a computer and a screen on which the results from the HCP measurements are displayed. (c) Part of the screen available for assessment by the healthcare professional. The two black dotted rectangles are not visible on the screen but serve to indicate the location on the screen of the continuously moving graphs of the 12-lead ECG (top rectangle), and the biventricular VTC (bottom rectangle) as assessed by the HCP algorithm (Konings *et al* 2012).

potential application range, because it can be used for home monitoring or monitoring in the hospital while performing light activities from everyday life, such as walking up a flight of stairs.

All HCP measurements were performed according to HCP standard operation procedures. In short, we applied the four current-applying HCP electrodes (Nutrode-P20M0, Nutrode-P10M0 pre-gelled, GE Healthcare, United Kingdom) on the hips and above the left and right clavicle. The electrode patch containing the six independent electrode pairs was placed on the participant's thorax in a predefined pattern using two markers printed on the patch, i.e. a central vertical line on the patch to be aligned with the central vertical axis of the sternum, and a small lateral notch in the patch that must coincide with the 4th intercostal space. The exact location of the patch during HCP1 (pre-MRI) was marked on the skin in order to attach a second electrode patch at exactly the same position during the HCP2 measurement (post-MRI). All HCP measurements were performed in supine position with normal resting breathing rate. Each HCP measurement session took approximately 10 min.

2.3. MRI protocol and image analyses

MRI in supine position at rest was performed with a 3T MR system (Ingenia; Philips, The Netherlands). After scout imaging, a stack of 15–20 contiguous left-ventricular short-axis views was acquired covering the entire LV

and RV from apex to above the base. Cinematographic images were acquired during end-expiratory breath-holds using retrospective ECG-triggering at a relatively high temporal resolution of 15 ms/frame. Other parameters: balanced steady-state free precession sequence; repetition time/echo time, 2.8/1.4 ms; SENSE factor, 2; field of view, 300 × 300 mm; slice thickness, 8 mm. Total MR examination time was approximately 30 min. Quantification of left- and right-ventricular volumes throughout the cardiac cycle was performed via endocardial contouring (cvi42, version 5; Circle Cardiovascular Imaging Inc., Canada), yielding LV and RV end-diastolic volumes (EDV), end-systolic volumes (ESV), stroke volumes (SV), ejection fractions (EF), and LV- and RV-VTCs.

Due to electromagnetic interference, the HCP cannot be used inside an MR scanner. HCP measurements were performed twice, i.e. a first HCP measurement within 20 min before the MRI measurement (HCP1), and a second HCP measurement immediately after the MRI measurement (HCP2). Participants were instructed to not drink and abstain from using the bathroom from the start of the HCP1 measurement until the completion of the HCP2 measurement after MRI examination to reduce the potential impact of any physiological differences between HCP and MRI measurements.

2.4. Statistical methods

To assess accuracy of the HCP, ICCs between LV-VTCs and RV-VTCs measured by HCP and MRI were calculated for all participants. ICCs between three pairs (a, b, c) of biventricular VTCs with equal R–R interval measured by HCP1 and HCP2 were calculated for each study participant to assess repeatability of HCP VTCs' morphology. ICCs were determined using a two-way random effects model with absolute agreement; single measures are reported, and values are interpreted as poor (<0.40), fair (0.40–0.59), good (0.60–0.74), and excellent (0.75–1.00) (Cicchetti 1994).

The HCP-VTC with an R–R interval length most similar to that of the MRI acquisitions was selected for the comparison regardless of whether this measurement was from HCP1 or HCP2. To allow comparison of HCP-VTC data measured at sample rate of 5 ms with MRI-VTC data measured at a temporal resolution of 15 ms, the HCP-VTC data were downsampled. In addition, since each HCP-VTC represents volume changes as a percentage of SV, the ventricular volumes in each MRI-VTC graph were expressed as a percentage of SV as well.

To perform a detailed analysis of relevant clinical parameters of systolic and diastolic cardiac function, values of these parameters were derived from VTCs and compared between HCP and MRI. Parameters describing ventricular volumes in time were calculated from the original VTC (figure 2(a)) and the time-derivative (figure 2(b)). The parameters tSys and isovolumetric relaxation time (IVRT) were based on the time-derivative: the period around the zero-crossing between (±0.25 × early Peak Filling Rate (PFR)) was defined as the IVRT. IVRT is by definition in diastole. 1/3FF measures were based on one-third of the filling period following the IVRT. *E*/*A* ratio was defined as the ratio of early PFR (ePFR) to atrial PFR (aPFR).

Bland–Altman plots (Bland and Altman 1986, Giavarina 2015) were used to assess the agreement between measurement of HCP- and MRI-VTC parameters such as tSys, 1/3FF and *E*/*A* ratio. The measurement agreement between HCP and MRI was determined by calculating the bias (mean difference between methods) and the standard deviation (SD) of the differences with lower and upper limits of agreement (LOA) (i.e. bias ± 1.96 × SD). Additionally, to assess HCP precision in terms of measurement repeatability of tSys and 1/3FF of biventricular VTCs, we compared the values for the parameters (mean ± SD) of six measurements of HCP1 and HCP2 for each study participant and calculated the coefficient of variations (CV) and repeatability coefficient. The CV is the ratio of the standard deviation over the mean (SD/mean × 100). The inter-session repeatability coefficient (CR) (i.e. 1.96 × SD of the intrasubject differences of the mean for HCP1 and HCP2) was determined for measurement of each parameter (Bland and Altman 1986, Bunting *et al* 2019). All statistical analyses were performed using IBM SPSS Statistics version 22.0 and GraphPad Prism version 9.4.1. Data are reported as mean (range) or mean (SD).

3. Results

3.1. Study participant characteristics

Six healthy study participants (male/female, 5/1), free from cardiovascular disease, underwent HCP and MRI measurements. Mean age was 32 (24–62) years. Mean BMI was 24.8 (21.6–27.7) kg m^{-2}.

The individual volumetric parameters of the six study participants measured by MRI are presented in table 1. The LV–SV ranged from 124.1–129.8 mL, RV–SV 103.4–132.1 mL, LV ejection fraction (EF) 54.8%–61.1% and RV EF 51.1%–56.7%.

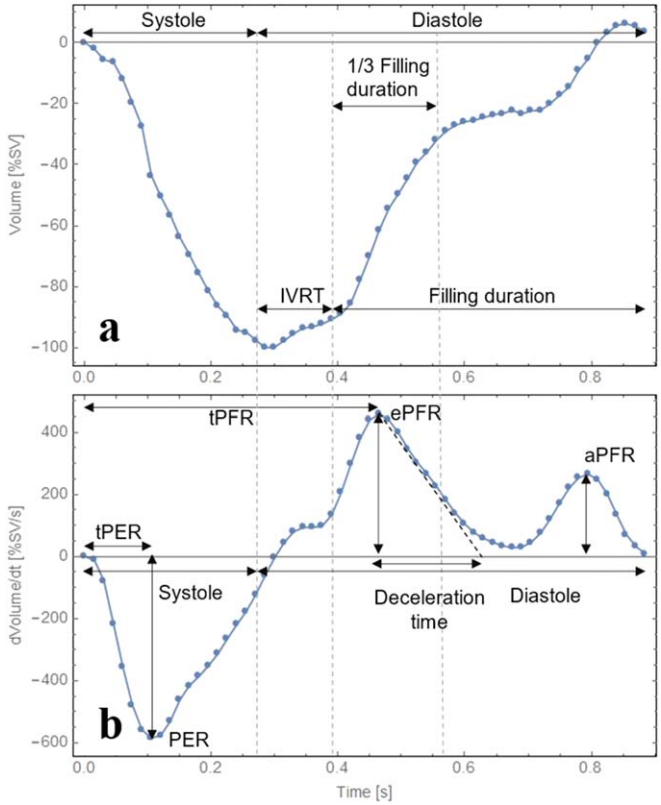

Figure 2. Definition of volume-time curve (VTC) parameters based on the relative VTC, using MRI data of one of the study participants as an example. In (a) the relative volume change [as a percentage of the stroke volume (SV)] is shown and in (b) the time-derivative of (a) is rendered. The volume change (expressed as a percentage of the SV) at the moment in time that one-third of the filling duration has taken place (i.e. at the end of the 1/3 filling duration), defines the 1/3 filling fraction (1/3FF). In this example, 1/3FF equals approximately 78% of the SV. PER indicates peak ejection rate, tPER: time to peak ejection rate, ePFR: early peak filling rate, aPFR: atrial peak filling rate, tPFR: time to peak filling rate, IVRT: isovolumetric relaxation time.

Table 1. Magnetic resonance imaging (MRI) measurements of ventricular volumes per study participant.

	Study participant	1	2	3	4	5	6
EDV (mL)	LV	203.1	214.4	233.7	223.5	225.8	170.1
	RV	221.8	221.8	235.7	233.2	228.4	167.7
ESV (mL)	LV	78.9	84.6	105.7	96.9	96.4	57.8
	RV	108.5	96.6	103.5	109.3	98.8	64.3
SV (mL)	LV	124.1	129.8	128.0	126.6	129.4	112.3
	RV	113.3	125.2	132.1	123.9	129.5	103.4
EF (%)	LV	61.1	60.5	54.8	56.6	57.3	66.0
	RV	51.1	56.5	56.1	53.1	56.7	61.7
CO (L/min)	LV	7.0	8.8	8.4	8.9	7.3	6.2
	RV	6.4	8.5	8.7	8.7	7.3	5.7
tSys (ms)	LV	350.9	297.5	322.8	294.2	278.7	314.8
	RV	382.2	303.3	347.2	320.5	358.3	323.8
1/3FF (%SV)	LV	71.3	59.8	41.0	77.5	78.9	84.7
	RV	48.3	41.9	33.3	49.5	66.1	71.2
E/*A* ratio	LV	1.8	2.1	1.6	3.9	3.0	3.9
	RV	0.8	0.9	0.7	1.4	1.1	1.8

EDV: end-diastolic volume, ESV: end-systolic volume, SV: stroke volume, EF: ejection fraction, CO: cardiac output, tSys: systolic time, 1/3FF: 1/3 filling fraction, *E*/*A* ratio: ratio of early € and atrial (A) filling, LV: left ventricle, RV: right ventricle.

3.2. HCP validation

3.2.1. Comparison of HCP-VTC against MRI-VTC

Figures 3 and 4 present VTCs of LV and RV, respectively, for all study participants, as measured by HCP and MRI. All HCP-VTCs demonstrated good morphological agreement with MRI-VTCs during the systolic and the

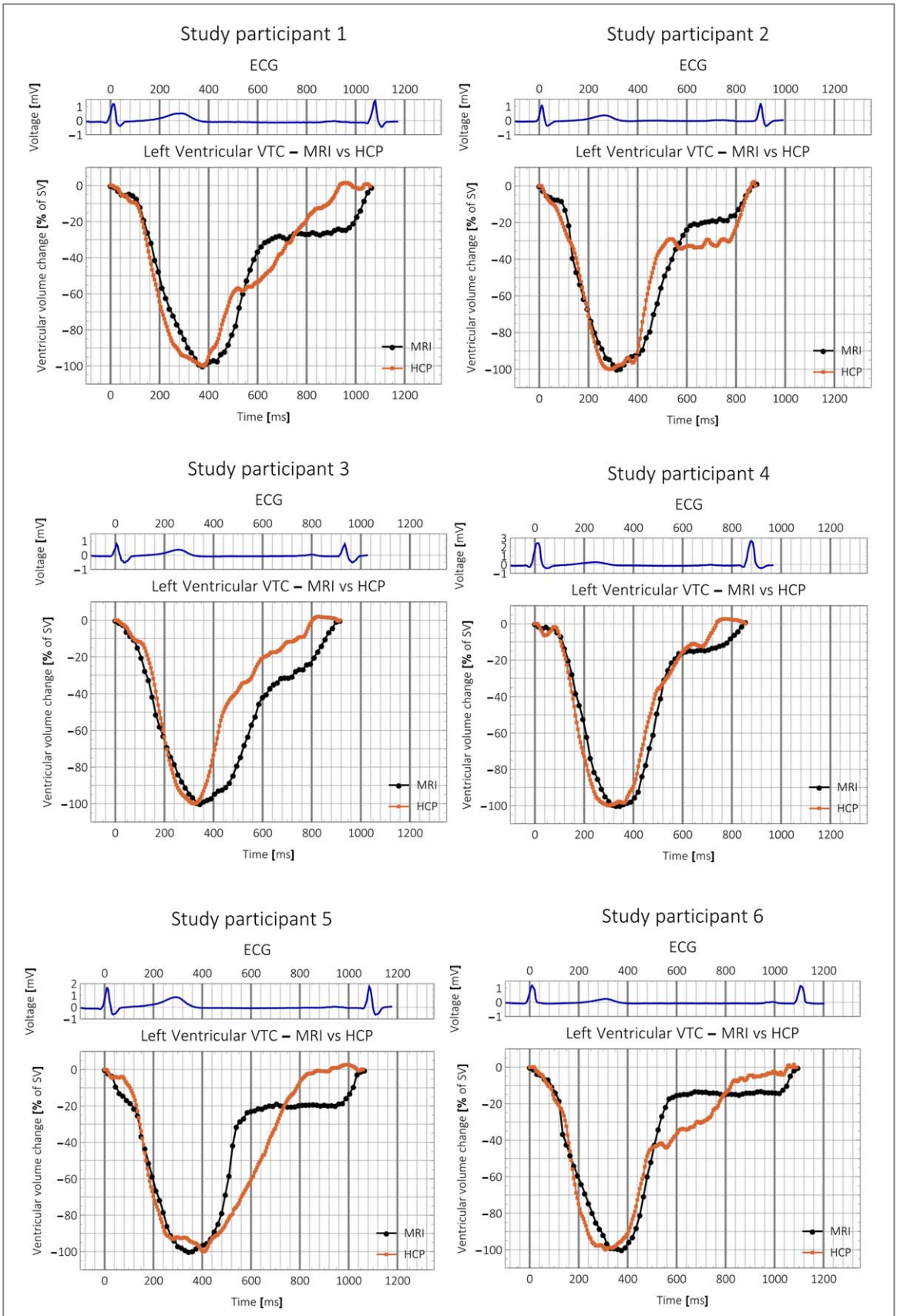

Figure 3. Left-ventricular volume-time curves (VTCs) of MRI versus hemodynamic cardiac profiler (HCP) of all study participants, together with corresponding ECG from HCP.

rapid filling phases. We observed small deviations between HCP-VTC and MRI-VTC during diastasis, for both LV and RV.

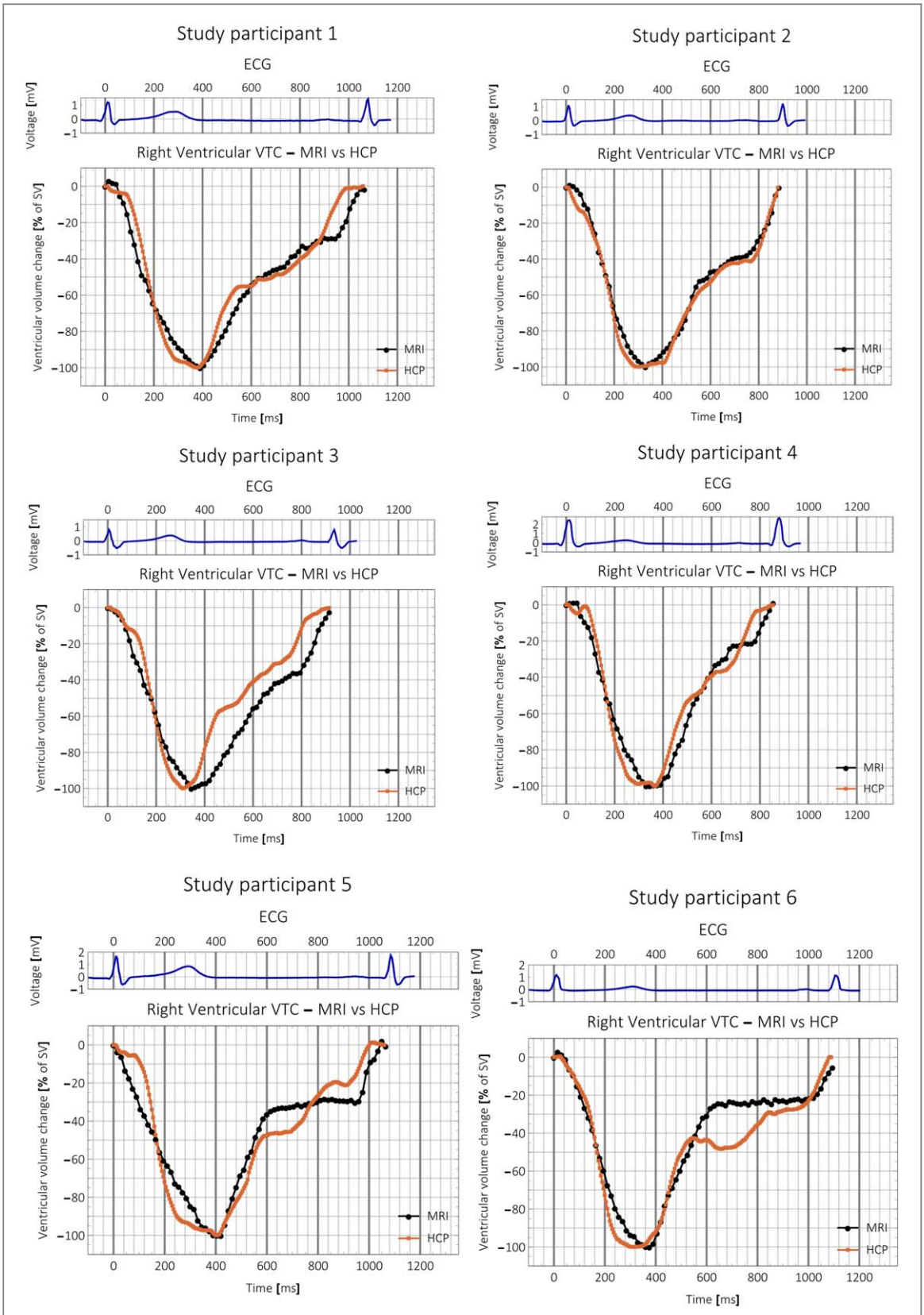

Figure 4. Right-ventricular volume-time curves (VTCs) of MRI versus Hemodynamic Cardiac Profiler (HCP) of all study participants, with corresponding ECG from HCP.

3.2.2. Intraclass correlation coefficients between MRI-VTCs and HCP-VTCs

The ICCs between MRI-VTCs and HCP-VTCs are shown in table 2. All ICCs were $\geqslant 0.8$, indicating excellent agreement between MRI-VTC and HCP-VTC. Mean (range) ICC of HCP LV-VTC versus MRI LV-VTC was 0.91 (0.80–0.96). Mean (range) ICC of RV-VTC was 0.94 (0.88–0.99).

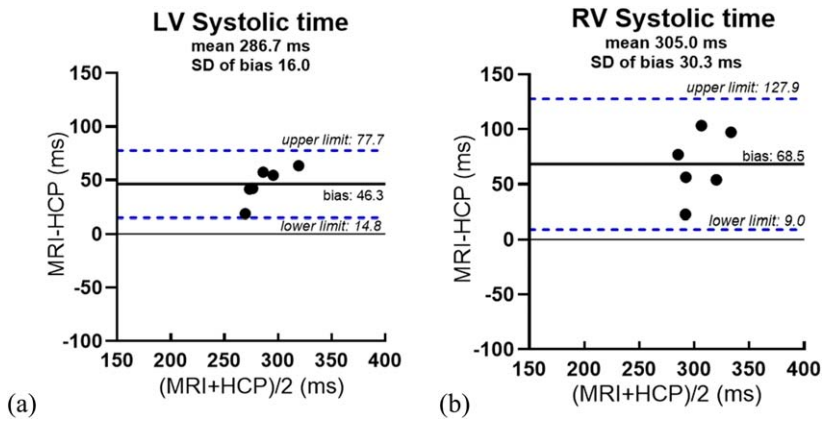

Figure 5. (a) Bland–Altman plot on the measurement agreement of systolic time (tSys (ms)) of the left ventricle (LV) between MRI and the Hemodynamic Cardiac Profiler (HCP). Mean bias was 46.3 ± 16.0 ms with lower and upper LOA of 14.8 ms and 77.7 ms respectively at a mean value of 286.7 ± 30.9 ms. (b) Bland–Altman plot on the agreement of measurement of tSys (ms) of the right ventricle (RV) between MRI and HCP. Mean bias was 68.5 ± 30.3 ms with lower and upper limits of agreement of 9.0 ms and 127.9 ms respectively at a mean value 305.0 ± 42.5 ms.

Table 2. Intraclass correlation coefficients between MRI and HCP volume-time curves.

Study ID	Comparison MRI versus HCP	Heart rate		n	ICC (95% CI)[a]
		MRI	HCP		
1	LV	56.3	56.6	71	0.922 (0.877–0.950)
	RV	56.3	56.6	71	0.960 (0.929–0.976)
2	LV	67.8	68.2	59	0.944 (0.907–0.966)
	RV	67.8	68.2	59	0.989 (0.965–0.995)
3	LV	65.6	65.6	61	0.800 (0.173–0.928)
	RV	65.6	65.6	61	0.876 (0.391–0.956)
4	LV	70.2	70.2	57	0.962 (0.936–0.977)
	RV	70.2	70.2	57	0.966 (0.942–0.980)
5	LV	56.3	56.3	71	0.890 (0.829–0.930)
	RV	56.3	56.3	71	0.933 (0.894–0.958)
6	LV	54.8	55.0	73	0.941 (0.908–0.963)
	RV	54.8	55.0	73	0.937 (0.865–0.967)

[a] Two-way random effects model with absolute agreement (single values).
ICC indicates intraclass correlation coefficient, n: datapoints within single VTC, LV: left ventricle, RV: right ventricle, CI: confidence interval.

3.2.3. VTC-derived parameters of HCP versus MRI: Bland–Altman analyses

Bland–Altman analyses of the VTC-derived parameters tSys (ms), 1/3FF (% SV) and *E*/*A* ratio for LV and RV comparing values measured by HCP and MRI are shown in figures 5(a) and (b), figures 6(a) and (b) and figures 7(a) and (b) respectively.

The bias ±SD for LV tSys was 46.3 ± 16.0 ms with lower and upper limits of agreement (LLOA and ULOA) of 14.8 ms and 77.7 ms at a mean value of 286.7 ± 30.9 ms (figure 5(a)), whereas the bias ± SD for RV tSys was 68.5 ± 30.3 ms (LLOA: 9.0 ms and ULOA: 127.9 ms) at a mean value of 305.0 ± 42.5 ms (figure 5(b)). The bias ± SD for LV 1/3FF was 8.2 ± 20.6 %SV (LLOA: −32.3 %SV and ULOA: 48.6 %SV) at a mean value of 64.8 ± 13.3 %SV (figure 6(a)), whereas the bias ± SD for RV 1/3FF was 3.7 ± 11.1 %SV (LLOA: −18.0 %SV and ULOA: 25.3 %SV) at a mean value of 49.9 ± 10.7% (figure 6(b)). The bias ± SD for LV E/A ratio was 0.13 ± 0.87 (LLOA: −1.6 and ULOA: 1.8) at a mean value of 2.65 ± 0.86 (figure 7(a)), whereas the bias ± SD for RV *E*/*A* ratio was −0.23 ± 0.35 (LLOA: −0.9 and ULOA: 0.5) at a mean value of 1.23 ± 0.39 (figure 7(b)).

3.3. HCP repeatability

3.3.1. Intraclass correlation coefficients between biventricular VTCs of HCP1 and HCP2

Table 3 shows the ICCs and 95% confidence intervals (CI) of repeatability of HCP VTCs' morphology. Pre- and post-MRI measurements (HCP1 and HCP2) were similar. ICCs between three pairs (a, b, c) of

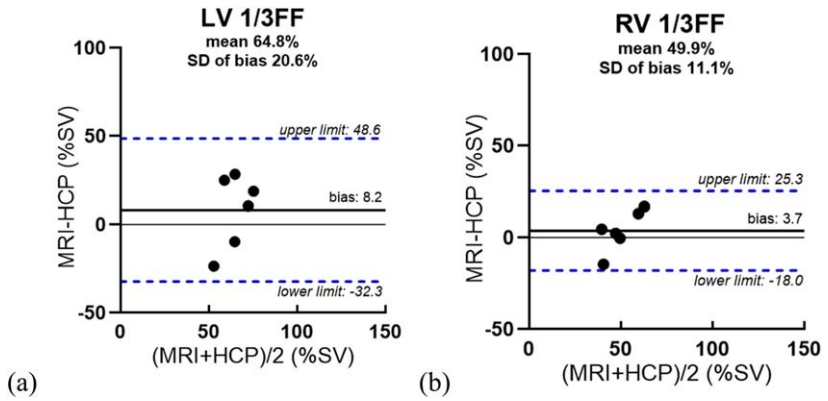

Figure 6. (**a**) Bland–Altman plot on the measurement agreement of one-third filling fraction (1/3 FF (%SV)) of the left ventricle (LV) between MRI and the Hemodynamic Cardiac Profiler (HCP). Mean bias was 8.2 ± 20.6 %SV with lower and upper limits of agreement of −32.3 %SV and 48.6 %SV respectively at a mean value of 64.8 ± 13.3 %SV. (**b**) Bland–Altman plot on the agreement of measurement of 1/3 FF (%SV) of the right ventricle (RV) between MRI and HCP. Mean bias was 3.7 ± 11.1 %SV with lower and upper limits of agreement of −18.0 %SV and 25.3 %SV respectively at a mean value of 49.9 ± 10.7 %SV.

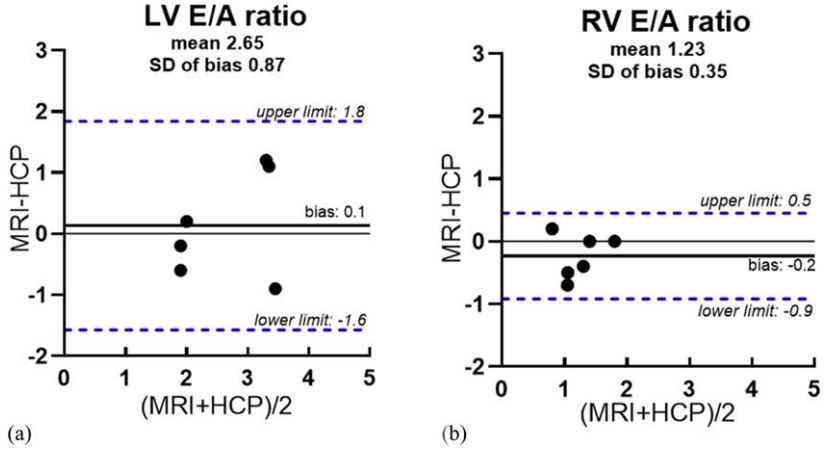

Figure 7. (**a**) Bland–Altman plot on the measurement agreement of the ratio of the volumes of the early (*E*) and late (*A*) left ventricular diastolic filling (*E*/*A* ratio) between MRI and the Hemodynamic Cardiac Profiler (HCP). Mean bias was 0.1 ± 0.87 with lower and upper limits of agreement of −1.6 and 1.8 respectively at a mean value of 2.65 ± 0.86. (**b**) Bland–Altman plot on the agreement of measurement of RV *E*/*A* ratio between MRI and HCP data. Mean bias was −0.23 ± 0.35 with lower and upper limits of agreement of −0.9 and 0.45 respectively at a mean value of 1.23 ± 0.39.

biventricular VTCs of HCP1 (pre-MRI) and HCP2 (post-MRI) per study participant ranged from 0.907 to 0.995 for all study participants, indicating excellent agreement and repeatability of HCP-VTCs' morphology. An example of HCP1 (pre-MRI) and HCP2 (post-MRI) VTCs with equal R–R interval is shown in figure 8 (study participant #2).

3.3.2. VTC-derived parameters of HCP1 versus HCP2

A comparison between VTC-derived parameters tSys (ms), 1/3 FF (%SV) for biventricular VTCs measured by HCP1 and HCP2 are shown in figure 9 and figure 10, respectively. Additionally, heart rate (bpm) of HCP1 and HCP2 for each study participant is shown in figure 11. Table 4 shows HCP's measurement of agreement between values (mean ± SD of 6 biventricular VTCs of HCP1and HCP2) for tSys, 1/3FF and heart rate of measurement HCP1 and HCP2. The repeatability coefficient (CR) for measurement of tSys is ± 45.0 ms at a mean value of 282.9 ± 26.3 ms. The values of observed differences (HCP2-HCP1) for tSys (−35.7, −2.2, 21.8, 15.3, −18.0, 18.1 ms) are within the subscale's mean error (± 45.0 ms), suggesting that all observed differences do not reflect real differences but are differences considered to belong to measurement error (Vaz *et al* 2013).

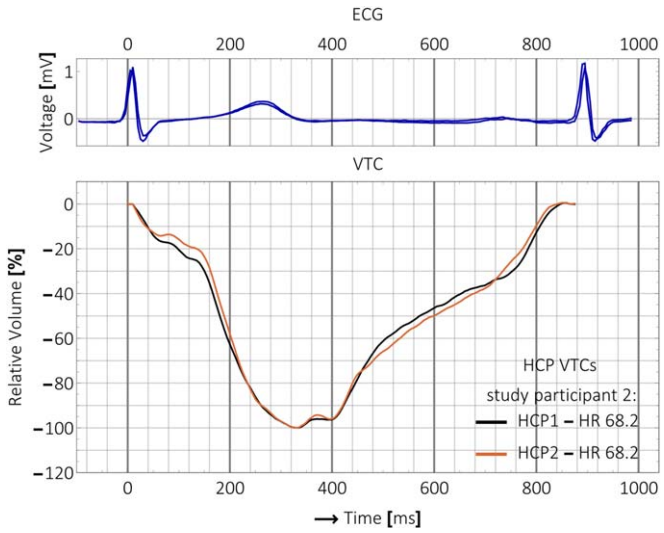

Figure 8. Biventricular volume-time curves obtained before (HCP1) and immediately after (HCP2) MRI examination with corresponding R-R intervals (ECG (top): −/+ 100 ms at start and end respectively) of study participant #2. Intraclass correlation coefficient (95% confidence interval): 0.995 (0.993–0.996).

Table 3. Intraclass correlation coefficients and 95% CI of HCP repeatability.

Study ID	VTC pairs HCP1—HCP2	Heart rate HCP1—HCP2	HCP1 versus HCP2, n datapoints in VTC	ICC (95% CI)[a]
1	a	57.1–57.1	211–211	0.907 (0.688–0.958)
	b	56.6–56.6	213–213	0.930 (0.857–0.960)
	c	56.1–56.1	215–215	0.871 (0.642–0.938)
2	a	68.2–68.2	176–176	0.995 (0.993–0.996)
	b	68.2–68.2	176–176	0.992 (0.989–0.994)
	c	64.2–64.2	187–187	0.992 (0.960–0.997)
3	a	63.8–63.8	189–189	0.966 (0.955–0.975)
	b	62.2–62.2	194–194	0.966 (0.955–0.974)
	c	61.9–61.9	195–195	0.944 (0.889–0.968)
4	a	68.6–69.4	175–173	0.987 (0.959–0.994)
	b	71.4–67.4	168–178	0.987 (0.971–0.993)
	c	70.2–67.4	171–178	0.973 (0.513–0.992)
5	a	52.2–52.6	229–231	0.987 (0.983–0.990)
	b	53.3–54.8	225–219	0.958 (0.925–0.974)
	c	56.1–54.5 (51.5)	215–233	0.969 (0.943–0.981)
6	a	54.8–54.8	219–219	0.928 (0.893–0.950)
	b	52.2–52.2	230–230	0.663 (0.271–0.822)
	c	50.4–50.6	238–237	0.832 (0.669–0.902)

[a] Two-way random effects model with absolute agreement (single values).
ICC indicates intraclass correlation coefficient, CI: confidence interval.

4. Discussion

In this pilot validation and repeatability study in healthy participants, we found agreement between VTCs from HCP and VTCs from MRI, both for the LV and RV. This agreement between VTCs from HCP and VTCs from MRI suggests VTCs produced by HCP may be a promising alternative for measuring VTCs by MRI.

Visual inspection of HCP-VTCs revealed a consistent similarity to MRI-VTCs during the systolic phase and the rapid filling phase. However, during diastasis, for both ventricles, HCP-VTCs demonstrated slightly more visual deviations from the MRI-VTCs. Although ICCs are generally high for all participants, this does not necessarily imply that the measurements agree in all individual cases. For instance, not all participants show a strong agreement of HCP-VTCs with MRI-VTCs.

The measurement accuracy of the current version of the HCP appears to be capable of detecting major deviations during systole and early diastole This is confirmed by Bland–Altman analysis of tSys (which is an important parameter of systolic function) as well as by Bland–Altman analysis of 1/3FF of the right ventricle

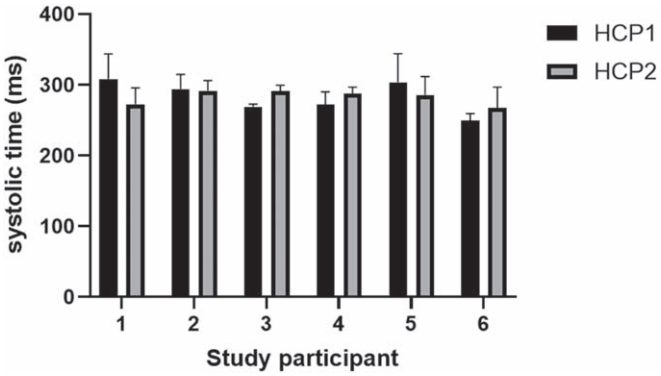

Figure 9. HCP measurement repeatability of systolic time (tSys [ms]). Bars indicate the mean tSys value of 6 biventricular VTCs from either HCP1 (left bar) or HCP2 (right bar) for each study participant. Whiskers indicate standard deviation.

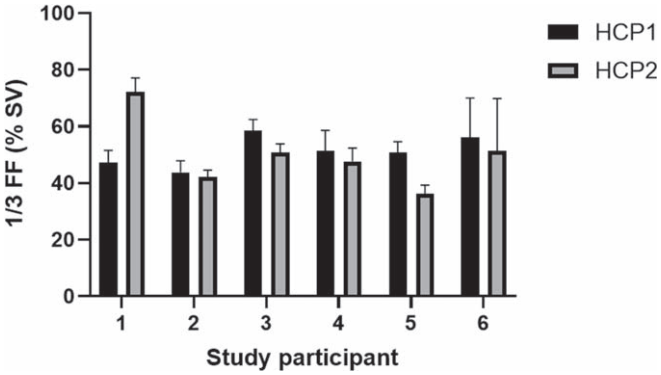

Figure 10. HCP measurement repeatability of one-third filling fraction (1/3 FF [% SV]). Bars indicate the mean 1/3FF value of 6 biventricular VTCs from either HCP1 (left bar) or HCP2 (right bar) for each study participant. Whiskers indicate standard deviation.

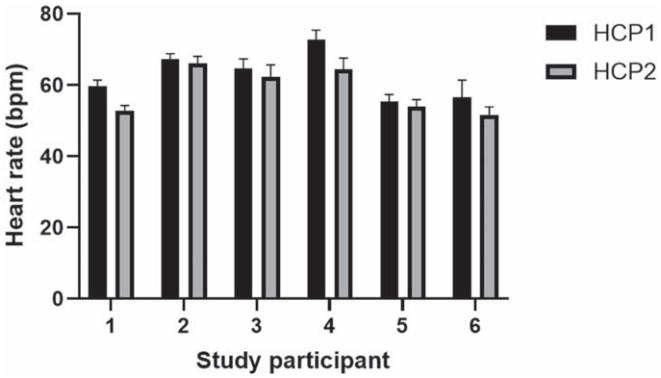

Figure 11. HCP measurement repeatability of heart rate (bpm). Bars indicate the mean heart rate value of 6 biventricular VTCs from either HCP1 (left bar) or HCP2 (right bar) for each study participant. Whiskers indicate standard deviation.

(which is an important parameter during the first stage of the diastole and may help detecting reduced diastolic function) (Zoghbi *et al* 1990). The Bland–Altman plots for the E/A ratio reveal broad limits of agreement. Because E/A is a ratio, the exact value of E/A becomes numerically very sensitive to variations in small values of A in the denominator.

Measurement repeatability of the morphology of biventricular VTCs was excellent for all six study participants. This is particularly relevant for situations in which the HCP is used to either (i) perform repeated HCP measurements on the same patient over the course of time (days, weeks, months) for monitoring purposes, such as during recovery from an intervention or after initiation or discontinuation of medication (e.g. cardiotoxicity of certain cancer medications, heart failure medication, etc) (Schimmel *et al* 2004, Asnani and

Table 4. Precision of HCP's measurement of volume time curve-derived parameters.

Parameter	Study participant	Number of VTCs	HCP1 Mean (SD)	CV (%) HCP1	Number of VTCs	HCP2 Mean (SD)	CV (%) HCP2	Difference of the mean *(HCP2-HCP1)*	Repeatability coefficient
tSys (ms)	1	6	308.6 (35.4)	11.48	6	272.9 (23.1)	8.46	−35.7	
	2	6	294.1 (20.6)	7.01	6	291.9 (14.2)	4.86	−2.2	
	3	6	269.3 (3.4)	1.28	6	291.1 (8.4)	2.87	21.8	
	4	6	272.4 (17.7)	6.51	6	287.7 (9.3)	3.22	15.3	
	5	6	303.8 (40.2)	13.25	6	285.8 (26.0)	9.11	−18.0	
	6	6	249.4 (10.2)	4.07	6	267.5 (29.2)	10.92	18.1	
Mean (SD)								−0.1 (23.0)	63.8
1/3FF (% SV)	1	6	47.3 (4.2)	8.91	6	72.1 (5.0)	6.94	24.8	
	2	6	43.8 (4.1)	9.28	6	42.1 (2.4)	5.70	−1.7	
	3	6	58.4 (4.0)	6.92	6	50.8 (3.1)	6.13	−7.6	
2	4	6	51.4 (7.2)	14.11	6	47.6 (4.8)	10.06	−3.8	
	5	6	50.8 (3.8)	7.47	6	36.2 (3.1)	8.66	−14.7	
	6	6	56.1 (14.0)	24.91	6	51.5 (18.4)	35.79	−4.6	
Mean (SD)								−1.3 (13.5)	37.4
Heart rate (bpm)	1	6	59.6 (1.8)	3.03	6	52.9 (1.4)	2.63	−6.7	
	2	6	67.3 (1.6)	2.32	6	66.0 (2.1)	3.18	−1.3	
	3	6	64.7 (2.7)	4.16	6	62.2 (3.5)	5.60	−2.5	
	4	6	72.7 (2.7)	3.76	6	64.4 (3.2)	5.03	−8.3	
	5	6	55.4 (2.0)	3.55	6	53.9 (2.0)	3.79	−1.5	
	6	6	56.6 (4.8)	8.52	6	51.5 (2.4)	4.67	−5.1	
Mean (SD)								−4.2 (2.9)	8.0

SD: standard deviation, CV: Intra-session coefficient of variation, tSys: systolic time, 1/3FF: 1/3 filling fraction, *E*/*A* ratio: ratio of early (E) and atrial (A) filling.

Peterson 2017). Furthermore, the equivalence of HCP1 and HCP2 also serves as a further a posteriori accountability for the chosen method of selecting a VTC from the HCP measurements on the basis of having a heart rate close to the heart rate as measured in the MRI, regardless of whether the HCP measurement was performed before or after MRI. We have assessed the variation of the heart rate during the MRI measurements on the basis of the RR-intervals of the ECG that was recorded simultaneously inside the MR system. This yielded a standard deviation of 9.6 bpm. The precision of HCP's measurement of the parameter tSys is in the same order of magnitude of the effect size that is seen in patients with heart failure relative to normal subjects (Reant *et al* 2010, Patel *et al* 2020). For the left ventricle, precision of HCP's measurement of 1/3FF was substantially lower compared to what is reported for the Doppler-based values of RV or LV assessments in a normal population (Zoghbi *et al* 1990), but is currently not suitable for reliably selecting patients with cardiomyopathy, coronary disease (Lavine *et al* 1985) or HFpEF (Von Roeder *et al* 2017). For the right ventricle, however, the HCP's 1/3FF measurements were better than the HCP's 1/3FF measurements of the left ventricle.

4.1. Potential applications

Changes in systolic time and 1/3FF constitute important (early) signs of numerous groups of cardiac disease, such as heart failure with preserved or reduced ejection fraction (Lavine *et al* 1985, Reant *et al* 2010, Riesenkampff *et al* 2010, Von Roeder *et al* 2017, Patel *et al* 2020). Furthermore, concerning the diagnostic value of 1/3FF during early diastole, Montalescot *et al* indicated that impaired diastolic filling can be a first sign of myocardial ischemia (Montalescot *et al* 2013), and VTC-derived parameters for diastolic function have been shown to be well correlated with the severity of ischemia (Nakae *et al* 2008), myocardial infarction (Mendoza *et al* 2010) and heart failure with preserved ejection fraction (HFpEF) (Von Roeder *et al* 2017). Hence, our results indicate that the HCP may potentially be a useful diagnostic screening tool.

Whereas the HCP is intended to be a screening or monitoring tool, we do *not*, however, intend or expect the HCP to evolve into an actual full replacement for imaging modalities such as MRI. Once the suspicion of the presence of (impending) cardiac disease in a specific individual is raised by the HCP in a more general, screening-like setting, this individual will need to be referred for further guideline-based diagnostics and management.

The current portable prototype of the HCP can measure and store VTC data for many hours in a row (up to 4 h), and is equipped with an 'event button', which can be pressed by the patient during episodes of discomfort (or exercise) to mark certain points in time linked to the corresponding VTCs, for easy reference by the cardiologist or other healthcare professionals. This is an advantage in comparison to echocardiography, which provides only a snapshot of the heart at a specific moment in time during the day, whereas a patient may experience cardiac discomfort during various moments during the day, but frequently not during the actual echocardiography.

4.2. Strengths and limitations

As the HCP technology stands now, reliable HCP measurements can be performed only if the patient is in a stable resting position (i.e. sitting on a chair in upright position, or lying down in supine position) *without* any movements apart from breathing. This is a limitation of the current technique of the HCP, which, however, can be remedied using the following strategy: in order to register the effect of e.g. walking up a flight of stairs, the patient needs to stand still for a minute directly after reaching the next floor, and to press the event button, thus registering the cardiac effects of walking up the stairs directly after the exertion itself. Nevertheless, even with this requirement to stand still after exertion, the HCP allows for the recording of more events than would be possible during a single session of echocardiography.

As has been mentioned in the introduction section, the portable HCP described in this paper is capable of producing both the left-ventricular VTC (LV-VTC) and right-ventricular VTC (RV-VTC), whereas previously the system was not capable of distinguishing between LV-VTC and RV-VTC, and each VTC was considered simply to be the average of the LV-VTC and RV-VTC. More refined analyses (of the technical aspects of the HCP measurement technique) have since then shown that the original biventricular or 'average' ventricular volume V_{BIV} as function of time t (in ms, during a single heartbeat) is actually approximately equal to:

$$V_{BIV}(t) = 0.25V_{LV}(t) + 0.75V_{RV}(t),$$

in which $V_{BIV}(t)$ is the 'averaged biventricular' volume as a function of time, $V_{LV}(t)$ is the LV-VTC and $V_{RV}(t)$ is the RV-VTC. The stronger contribution of V_{RV} to the 'averaged biventricular' volume V_{BIV} (see the factor 0.75 in the equation for the RV-VTC, as opposed to the 0.25 for the LV-VTC) is caused by the fact that the HCP electrodes on the thoracic skin are closer to the right ventricle than to the left ventricle. As a result, the reliability of the resulting RV-VTC is better than the reliability of the LV-VTC(t), because, on the basis of the equation directly above, the RV-VTC is already much closer to the biventricular VTC, and therefore the 'correction' needed to obtain RV-VTC from the biventricular VTC $V_{BIV}(t)$ is relatively small.

In the current portable HCP prototype, the assessment of both LV-VTC and RV-VTC from the above equation is executed on the basis of an additional measurement using another stimulus electrode, thus producing an extra set of independent input data for the HCP algorithm to balance the increased number of unknowns needed for the assessment of both LV-VTC and RV-VTC.

This additional measurement used for distinguishing between the left and right ventricles, however, does not yet offer the precision of the assessment of the biventricular $V_{BIV}(t)$ itself, and requires more development in future work. Particularly, the present study involved *healthy* study participants only, and the current algorithm processing the additional measurement assumed a fixed relation between LV-VTC and RV-VTC *during systole*. Further development of this additional measurement and its associated algorithm is therefore needed to be able to assess both LV-VTC and RV-VTC even in the case of severe cardiac pathologies, in which the assumption of a fixed relation between LV-VTC and RV-VTC during systole may not hold.

As explained above, however, the $V_{BIV}(t)$ from the equation above is already a good approximation of the RV-VTC, and the RV-VTC on itself seems to already have merit as an indicator for (impending) pathologies of the heart as a whole, because of the intimate relation between the volumetric motions of both ventricles (Maceira *et al* 2006, Borlaug and Kass 2009, Schwarz *et al* 2013, Vonk-Noordegraaf and Westerhof 2013, Vijiiac *et al* 2021).

This study has several limitations. First, the number of study participants was small. Furthermore, HCP and MRI measurements were not obtained at the same time, since it was impossible to use the HCP device in the MRI scanner due to electrical interference. Third, for highly reliable MRI-VTCs the protocol was limited to breath-hold acquisition, while HCP is principally designed to compute VTCs in the end expiratory phase from free-breathing data. This may contribute to morphological differences in VTCs between HCP and MRI. Other physiological conditions of study participants were kept stable and heart rate was similar during HCP and MRI measurements. In the specific case of the HCP, the VTC's and VTC-derived parameters are all calculated automatically in an operator-independent way, and, as a result, there was no interrater variability to be tested.

5. Conclusion

In this pilot study, HCP-VTCs were in agreement with MRI-VTCs. While this agreement was present for both the left and right ventricle, results for right-ventricular parameters showed generally better agreement than those for the left ventricle. Furthermore, repeatability of biventricular HCP-VTCs was excellent. Precision of HCP was good for measurement of systolic time. Findings for VTC-derived clinically relevant parameters, such as tSys and 1/3FF (for the right ventricle) indicate that the HCP may potentially become a useful non-invasive, low-cost and operator-independent screening tool for early detection of (impending) heart disease.

Data availability statement

All data that support the findings of this study are included within the article (and any supplementary information files).

ORCID iDs

Maurits K Konings https://orcid.org/0000-0003-1874-7201
Sjoerd M Verwijs https://orcid.org/0000-0003-3785-4985
Adrianus J Bakermans https://orcid.org/0000-0001-9291-9441
Harald T Jørstad https://orcid.org/0000-0003-3617-3256

References

Asnani A and Peterson R 2017 Cardiac toxicity of cancer chemotherapy *US Cardiol. Review* **11** 20–4
Barison A *et al* 2022 Cardiovascular magnetic resonance for the diagnosis and management of heart failure with preserved ejection fraction *Heart Fail. Rev.* **27** 191–205
Bland J M and Altman D G 1986 Statistical methods for assessing agreement between two methods of clinical measurement *Lancet* **327** 307–310
Borlaug B A and Kass D A 2009 Invasive hemodynamic assessment in heart failure *Heart Failure Clinics* **5** 217–28
Bunting K V *et al* 2019 A practical guide to assess the reproducibility of echocardiographic measurements *J. Am. Soc. Echocardiogr.* **32** 1505–15
Cicchetti D V 1994 Guidelines, criteria, and rules of thumb for evaluating normed and standardized assessment instruments in psychology *Psychol. Assess.* **6** 284–90
Giavarina D 2015 Understanding Bland Altman analysis *Biochem. Med.* **25** 141–51

Göransson C, Vejlstrup N and Carlsen J 2018 Reproducibility of peak filling and peak emptying rate determined by cardiovascular magnetic resonance imaging for assessment of biventricular systolic and diastolic dysfunction in patients with pulmonary arterial hypertension *Int. J. Cardiovasc Imaging* **34** 777–86

Konings M K *et al* 2012 A new electric method for non-invasive continuous monitoring of stroke volume and ventricular volume-time curves *Biomed. Eng.* **11** 51

Konings M K *et al* 2017 Non-invasive measurement of volume-time curves in patients with mitral regurgitation and in healthy volunteers, using a new operator-independent screening tool *Physiol. Meas.* **38** 241–58

Lavine S J *et al* 1985 Left ventricular diastolic filling in patients with coronary artery disease and normal left ventricular function *Am. Heart J.* **110** 318–25

Lima J A C and Desai M Y 2004 Cardiovascular magnetic resonance imaging: current and emerging applications *J. Am. Coll. Cardiol.* **44** 1164–71

Maceira A M *et al* 2006 Reference right ventricular systolic and diastolic function normalized to age, gender and body surface area from steady-state free precession cardiovascular magnetic resonance *Eur. Heart J.* **27** 2879–88

Mendoza D D *et al* 2010 Impact of diastolic dysfunction severity on global left ventricular volumetric filling - assessment by automated segmentation of routine cine cardiovascular magnetic resonance *J. Cardiovasc Magn. Reson.* **12** 46

Montalescot G *et al* 2013 ESC guidelines on the management of stable coronary artery disease: the task force on the management of stable coronary artery disease of the European society of cardiology *Eur. Heart J.* **34** 2949–3003

Nakae I *et al* 2008 Clinical significance of diastolic function as an indicator of myocardial ischemia assessed by 16-frame gated myocardial perfusion SPECT *Ann. Nucl. Med.* **22** 677–83

Patel P A *et al* 2020 Association between systolic ejection time and outcomes in heart failure by ejection fraction *Eur. J. Heart Fail.* **22** 1174–82

Reant P *et al* 2010 Systolic time intervals as simple echocardiographic parameters of left ventricular systolic performance: correlation with ejection fraction and longitudinal two-dimensional strain *Eur. J. Echocardiogr.* **11** 834–44

Riesenkampff E *et al* 2010 Integrated analysis of atrioventricular interactions in tetralogy of Fallot *Am. J. Physiol. Heart. Circ. Physiol.* **299** H364–71

Von Roeder M *et al* 2017 Influence of left atrial function on exercise capacity and left ventricular function in patients with heart failure and preserved ejection fraction *Circ. Cardiovasc Imaging* **10** e005467

Schimmel K J M *et al* 2004 Cardiotoxicity of cytotoxic drugs *Cancer Treat. Rev.* **30** 181–91

Schwarz K *et al* 2013 Right ventricular function in left ventricular disease: pathophysiology and implications *Heart Lung Circ.* **22** 507–11

Vaz S, Falkmer T, Passmore A E, Parsons R and Andreou P 2013 The case for using the repeatability coefficient when calculating test-retest reliability *PLoS One* **8** e73990

Vijiiac A *et al* 2021 Forgotten no more—the role of right ventricular dysfunction in heart failure with reduced ejection fraction: an echocardiographic perspective *Diagnostics* **11** 548

Vonk-Noordegraaf A and Westerhof N 2013 Describing right ventricular function *Eur. Respiratory J.* **41** 1419–23

Zoghbi W A, Habib G B and Quinones M A 1990 Doppler assessment of right ventricular filling in a normal population. Comparison with left ventricular filling dynamics *Circulation.* **82** 1316–24